Pseudochaotic poloidal transport in the laminar regime of the resistive ballooning instabilities

I. Calvo,[1] L. Garcia,[2] B. A. Carreras,[3] R. Sánchez,[4] and B. Ph. van Milligen[1]
[1]*Laboratorio Nacional de Fusión, Asociación EURATOM-CIEMAT, 28040 Madrid, Spain*
[2]*Universidad Carlos III, 28911 Leganés, Madrid, Spain*
[3]*BACV Solutions Inc., Oak Ridge, Tennessee 37830, USA*
[4]*Fusion Energy Division, Oak Ridge National Laboratory, Oak Ridge, Tennessee 37831, USA*

In toroidal geometry, and prior to the establishment of a fully developed turbulent state, the so-called topological instability of the pressure-gradient-driven turbulence is observed. In this intermediate state, a narrow spectral band of modes dominates the dynamics, giving rise to the formation of isosurfaces of electric potential with a complicated topology. Since $\mathbf{E}\times\mathbf{B}$ advection of tracer particles takes place along these isosurfaces, their topological complexity affects the characteristic features of radial and poloidal transport dramatically. In particular, they both become strongly nondiffusive and non-Gaussian. Since radial transport determines the system confinement properties and poloidal transport controls the equilibration dynamics (on any magnetic surface), the development of nondiffusive models in both directions is thus of physical interest. In previous work, a fractional model to describe radial transport was constructed by the authors. In this contribution, recent results on periodic fractional models are exploited for the construction of an effective model of poloidal transport. Numerical computations using a three-dimensional reduced magnetohydrodynamic set of equations are compared with analytical solutions of the fractional periodic model. It is shown that the aforementioned analytical solutions accurately describe poloidal transport, which turns out to be superdiffusive with index $\alpha=1$.

I. INTRODUCTION

Numerical calculations of resistive pressure-gradient-driven turbulence[1] in toroidal geometry show the existence of an unstable regime below the threshold for fully developed turbulence. In this regime, the toroidal mode spectrum in steady state is dominated by a single toroidal mode N. This dominant mode may fluctuate intermittently among a narrow range of possible values. For instance, with the parameters used in Ref. 1, $24\leq N\leq 26$. The transition from a stable plasma to this ballooning-mode-dominated regime has the characteristic properties of a topological instability.[2,3] After the transition, the isosurfaces of electrostatic potential induced by the ballooning modes have a complicated topological structure, which is a direct consequence of the (inner/outer) asymmetry in magnetic field strength inherent to any magnetic toroidal geometry. Consequently, particles advected by the $\mathbf{E}\times\mathbf{B}$ flows associated with these complex isosurfaces cease to behave diffusively. At this point, it is worth stressing that this situation is quite different from cases of near-critical turbulence discussed in the literature,[4] in which the nondiffusive nature of transport is related instead to the existence of spatiotemporal correlations between fluctuations and the background profile gradients from which they feed.

The structure of the potential isosurfaces can be visualized as we move in the toroidal direction around the torus, following the magnetic field lines. At the singular magnetic surfaces, (potential) vortices emerge with a structure which is consistent with the local twist of the magnetic field lines. As the outermost part of torus (the low-field side) is approached, filamentary vortices from different singular surfaces may merge and form extended radial streamers. Radial transport takes place predominantly within these streamers, since particles can freely travel along them in the radial direction. The nature of radial transport within these streamers characterizes the confinement properties of the system. As we continue to follow the lines toroidally, the vortices move back into the high-field side and the streamers break up. Each particle will then remain trapped within one of the filaments which emerge from this process. Poloidal (and toroidal) transport then follows, as the population of particles spreads out poloidally due to the free (ballistic) motion of each particle along the radially localized filament which contains it. Its nature thus determines how efficiently gradients are equilibrated on any magnetic surface. Eventually, some of the filaments will reach again the low-field side and merge to produce a new radial streamer, enabling again radial transport until the structure goes back in to the high-field side, brakes again up into new filaments, and ballistic poloidal spreading ensues again, and so on.

In Ref. 3 the radial transport of tracer particles in the unstable regime of this system was studied and found to be of a fractional, self-similar nature. This means that their transport can be described in terms of continuous-time random walks or fractional differential equations with appropriate exponents. It was also proven that the dynamics of tracers is pseudochaotic by showing that the dispersion of trajectories of (initially close) particles is polynomial (which in par-

ticular implies that the Lyapunov exponent is zero). In addition, an analogy between the topological structure of the flows and a billiard model (a paradigmatic example for pseudochaos) was discussed at length.

In this paper we focus instead on the construction of an effective transport model that captures the main features of poloidal transport. This task is much more than a simple academic exercise or a straightforward extension of the radial transport case. The reason is that the difference with the radial case is not only the different dominant physics, but the existence of a periodic boundary. In the radial case, an absorbing boundary exists at the plasma edge, which can be dealt with within the standard framework of fractional differential operators. It has not been until very recently that the mathematical framework necessary to deal with a periodic boundary has been worked out by deriving the fluid limit equations of a continuous-time random walk formulated on a circle.[5] In the numerical calculations of Ref. 1, the safety factor q was taken to be between 1 (at the plasma center) and 2 (at the plasma edge). Therefore, for a dominant toroidal mode N, there are $N+1$ possible filaments forming and the poloidal spreading of the tracers will take place in up to N finite-size steps in q. As N increases, the poloidal spreading of particle tracers should approach the results for a "fluid" transport model. In this paper, we will show that the new framework can deal successfully with the problem of poloidal transport in this system. It will also serve as illustration for future applications regarding transport along periodic directions in any magnetic configuration.

The rest of this paper is organized as follows: Sec. II gives a survey of the main results of Ref. 5 on continuous time random walks and the fractional diffusion equation formulated on the circle. In Sec. III we present the reduced magnetohydrodynamic model used in the study of the resistive pressure-gradient-driven turbulence and compare the numerical and analytical results for the transport of tracer particles. The conclusions are given in Sec. IV. The Appendix contains some basic definitions on stable Lévy distributions.

II. FRACTIONAL DIFFUSION EQUATION ON A CIRCLE

Continuous time random walks (CTRWs) (Refs. 6 and 7) are models describing the microscopic transport of particles in a probabilistic way. In this paper we are interested in the interpretation of poloidal transport in fusion plasmas as a CTRW defined on a circle. A general treatment of CTRWs on the circle has recently appeared.[5] In this section we collect the results of Ref. 5 which are relevant for the present work.

We denote by $n(\theta,t)$ the density of particles (tracer particles for the application of the formalism relevant to this paper) normalized to the total number of particles, i.e., $\int_0^{2\pi} n(\theta,t)\mathrm{d}\theta=1$, $\forall t$. The function $n(\theta,t)$ must be periodic in θ, $n(\theta+2\pi,t)=n(\theta,t)$. A separable, Markovian, homogeneous time-translational invariant CTRW is defined by a mean waiting time, τ, and a step-size pdf, $p(\Delta)$, giving the probability that a particle performs a jump from x to $x+\Delta$. The conservation of probability requires that $\int_{-\infty}^{\infty} p(\Delta)\mathrm{d}\Delta=1$. Since Δ runs over the interval $(-\infty,\infty)$, particles can wind around the circle an arbitrary number of times in each jump. We are interested in studying the case in which $p(\Delta)$ is a Lévy stable distribution (see the Appendix). When the index of stability $\alpha=2$, the pdf $p(\Delta)$ is Gaussian, whereas for $\alpha<2$ it has algebraic tails. One would expect that (at least) in the latter case the effect of the nontrivial topology of the circle be very relevant and the CTRW on the circle should exhibit significant differences with respect to a CTRW with the same step-size pdf formulated on the real line.

The dynamics described by the CTRW defined above is equivalent to the following generalized master equation (GME):[5]

$$\partial_t n(\theta,t) = \frac{1}{\tau}\int_0^{2\pi} \overline{p}(\theta-\theta')n(\theta',t')\mathrm{d}\theta' - \frac{n(\theta,t)}{\tau}, \tag{1}$$

with

$$\overline{p}(\theta) = \sum_{m=-\infty}^{\infty} p(\theta+2\pi m). \tag{2}$$

Notably, $\overline{p}$ is obtained from p by means of a ballooning transform.[8] The sum in Eq. (2) explicitly accounts for the aforementioned fact that, given $\theta,\theta'\in[0,2\pi)$, particles can arrive at θ from θ' through jumps of length $|\theta-\theta'+2\pi m|$, $m\in\mathbb{Z}$.

Consider the case of a step-size pdf given by a stable Lévy distribution (see the Appendix) with $\beta=0$, whose characteristic function is

$$\hat{p}(k) = \exp(-\sigma^\alpha|k|^\alpha + i\mu k). \tag{3}$$

Then, the fluid limit of the GME (1) is

$$\partial_t n = -\frac{\sigma^\alpha}{2\tau\cos(\pi\alpha/2)}({}_0\mathcal{D}_\theta^\alpha + {}^{2\pi}\mathcal{D}_\theta^\alpha)n + \frac{\mu}{\tau}\partial_\theta n, \tag{4}$$

where ${}_0\mathcal{D}^\alpha$ and ${}^{2\pi}\mathcal{D}^\alpha$ are the Riemann–Liouville operators on the circle derived in Ref. 5. The solution of Eq. (4) with initial condition $n(\theta,0)=\Sigma_{m=-\infty}^{\infty}\delta(\theta-2\pi m)$ (i.e., the propagator) is given by

$$n(\theta,t) = \frac{1}{2\pi}\sum_{m=-\infty}^{\infty} e^{(-\sigma^\alpha|m|^\alpha+i\mu m)t/\tau}e^{-im\theta}, \quad \alpha\in(0,2]. \tag{5}$$

In the limit $t\to\infty$, $n(\theta,t)\to 1/2\pi$, as required by the conservation of the number of particles.

When $\alpha=1$, which as we will see is the relevant case for the present work, the infinite sum on the right-hand side of Eq. (5) can be computed and a closed expression for the propagator can be obtained,

$$n(\theta,t) = \frac{1}{2\pi}\frac{\sinh(\sigma t/\tau)}{\cosh(\sigma t/\tau)-\cos(\mu t/\tau-\theta)}. \tag{6}$$

III. DYNAMICAL MODEL AND NUMERICAL CALCULATIONS OF TRACER PARTICLE TRANSPORT

In toroidal geometry, the underlying instability of the resistive pressure-gradient-driven turbulence is the so-called resistive ballooning mode.[9] To calculate the dynamical properties of these instabilities, we use the reduced set of magne-

tohydrodynamics equations[10,11] in toroidal geometry, and because of the low β values, we also use the electrostatic approximation. The model is then reduced to two equations: the perpendicular momentum balance equation and the equation of state. The former can be written in terms of the toroidal component of the vorticity U. In dimensionless form it reads

$$\frac{dU}{dt} = -S^2\mathbf{B}\cdot\nabla\left(\frac{R^2}{\eta F^2}\mathbf{B}\cdot\nabla\Phi\right) + S^2\frac{\beta_0}{\varepsilon^2}\frac{\mathbf{b}\times\boldsymbol{\kappa}}{B}\cdot\nabla p + \mu\nabla_\perp^2 U. \tag{7}$$

As for the equation of state,

$$\frac{dp}{dt} = D_\parallel\frac{R^2}{F}\mathbf{B}\cdot\nabla\left(\frac{R^2}{F}\mathbf{B}\cdot\nabla p\right) + D_\perp\nabla_\perp^2 p. \tag{8}$$

Here, $d/dt = \partial/\partial t + \mathbf{V}_\perp\cdot\nabla$ is the convective derivative, and

$$\mathbf{V}_\perp = -\frac{1}{B}\nabla\Phi\times\mathbf{b}, \tag{9}$$

where Φ is the electrostatic potential. There is a simple relation between the toroidal component of the vorticity and the stream function,

$$U = \frac{1}{B}\boldsymbol{\zeta}\cdot\nabla\times\mathbf{V}_\perp. \tag{10}$$

Therefore, we solve Eqs. (7) and (8) for p and Φ, taking into account Eqs. (9) and (10) to relate U and Φ. In Eq. (7), η is the plasma resistivity, $\mathbf{b}=\mathbf{B}/B$ is a unit vector in the direction of the magnetic field, and $\boldsymbol{\kappa}=\mathbf{b}\cdot\nabla\mathbf{b}$ is the magnetic field line curvature. The magnetic field is expressed as $\mathbf{B} = F\nabla\zeta + \nabla\zeta\times\nabla\psi$, where $F=RB_\zeta$ is the toroidal flux function, which is a very slowly varying function of the radial coordinate, r; ψ is the poloidal flux, which is not evolved in time, and ζ is the toroidal angle. Apart from the dissipation terms, we have two dimensionless parameters in these equations, $\beta_0 = p(0)/(B_\zeta^2/2\mu_0)$ and $S=\tau_R/\tau_{hp}$, the Lundquist number. Here, τ_R is the resistive time at the magnetic axis, $\tau_R = \mu_0 a^2/\eta(0)$, and τ_{hp} is the poloidal Alfvén time, $\tau_{hp} = R_0\sqrt{\mu_0 m_i n_0}/B_\zeta$, where m_i is the ion mass, and a and R_0 are the minor and major radius, respectively. In the above dynamical equations lengths are normalized to the minor radius a, and time to the resistive time τ_R.

To study the particle transport properties induced by these flow structures, we use pseudoparticles as tracers. These tracers are solutions of the equation of motion,

$$\frac{d\mathbf{r}}{dt} = \mathbf{V}_\perp(\mathbf{r},t) + V_0\mathbf{b}. \tag{11}$$

Here, the velocity is the flow velocity given by Eq. (9) in terms of the stream function, V_0 is an arbitrary velocity along the field line, and $\mathbf{b}=\boldsymbol{\zeta}-\boldsymbol{\theta}/q$. Since this model is electrostatic, all information on turbulence evolution comes through the electrostatic potential Φ. In the present calculations we will use a constant V_0 as an initial condition for the tracer particles and keep the velocity field frozen in time because we are only looking for the effect of the flow structure on the transport.

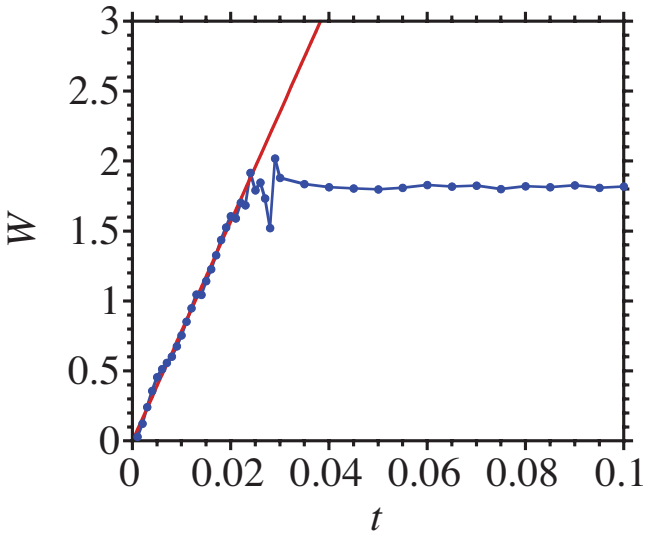

FIG. 1. (Color online) Standard deviation of the pdf of particle tracers vs time. The short-time behavior implies that the index α is equal to 1.

The first results of particle tracer transport have been obtained by launching 50 000 particles all with the same fixed initial velocity $V_0 = 400\pi$. At $t=0$ particles were located in a small region around $r=0.7$, $\theta=0$, and $\zeta=0$. The evolution is initially very asymmetric because of the preferential direction induced by the drift in the motion of the particles along the eddies, which are aligned with the field lines. However, as particles go several times around the torus, $n(\theta,t)$ becomes increasingly symmetric. For this reason, we first remove the drift of the distribution of tracers and then we compare the evolution with the symmetric solution of the fractional diffusion equation on the circle, Eq. (5).

The Lyapunov exponent in the motion of the particle tracers is zero and the trajectories separate from each other approximately linearly in time. Therefore, we expect α to be close to 1. Estimates based on simplified models give $\alpha \in [1.05, 1.11]$.[3,12] To test this assumption and to determine the value of α associated with the poloidal transport, we first look at the time evolution of the width of the distribution, i.e., the square root of the second moment of the particle distribution, $W(t)$. As shown in Fig. 1, $W(t)$ increases linearly with time until it saturates at a constant value, $W(\infty) = \pi/\sqrt{3}$, consistent with the flat tracer distribution. This behavior was expected from the analytical calculation. A fit of the data gives $\alpha = 0.984 \pm 0.027$, so that we can set $\alpha=1$. For the sake of completeness, we have plotted in Fig. 2 the time evolution of the first and third moments of the numerical pdf of tracers (after removing the drift), which are essentially zero at any time.

According to Eq. (6), the expected time evolution of the peak of the particle distribution is given by

$$n(0,t) = \frac{1}{2\pi}\frac{1+e^{-\sigma t/\tau}}{1-e^{-\sigma t/\tau}}. \tag{12}$$

By fitting this expression to the numerical data, we can determine the time decay constant σ/τ. The result of the fit is shown in Fig. 3, and the value of the constant is σ/τ

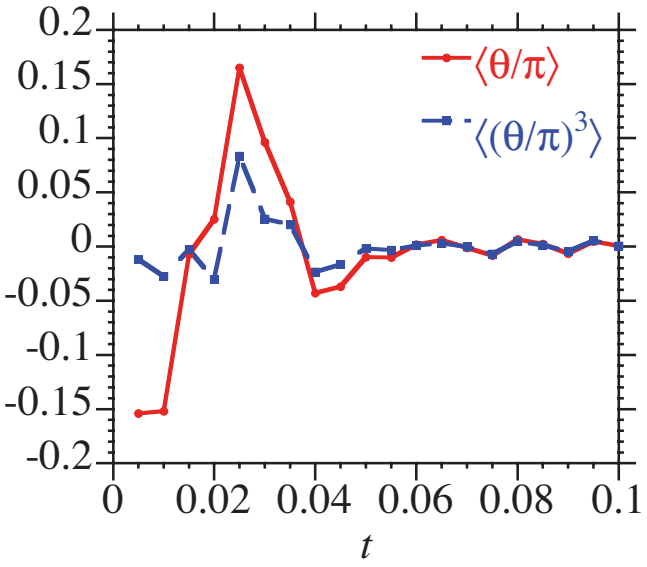

FIG. 2. (Color online) First and third moments of the pdf of particle tracers computed from the numerical integration of Eq. (11).

$=0.268\pm0.013$. Now, we can use the analytical expression for $n(\theta,t)$ given by Eq. (6) and compare this analytical prediction with the numerical data. We show a few examples of this comparison in Fig. 4. The analytical solution seems to describe the numerical results relatively well. Recall that Eq. (12) is derived from a CTRW with symmetric step-size pdf, hence the numerical distribution of tracers should have vanishing odd moments, as is indeed the case (see Fig. 2).

We have also calculated the time evolution of particle tracers with random initial velocities in the toroidal direction. We have used 50 000 particles and the results of a typical calculation showing the evolution of $n(\theta,t)$ are plotted in Fig. 5. In Fig. 5, one notes that the structures are gone. This is not surprising and it is one of the expected consequences

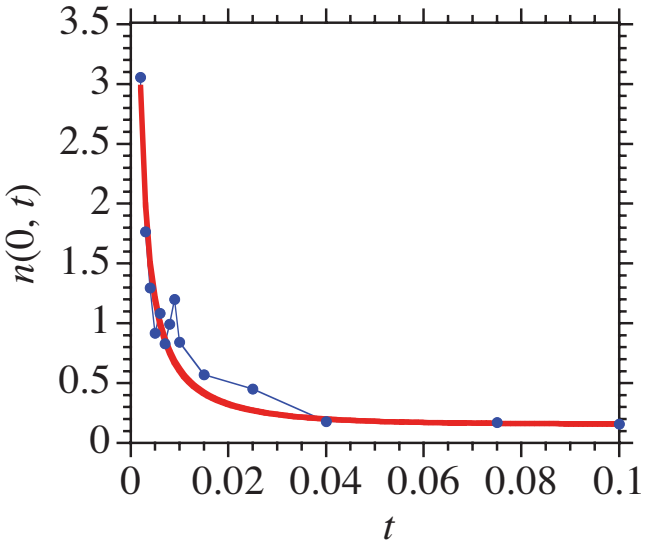

FIG. 3. (Color online) Numerical results for $n(0,t)$ obtained from Eq. (11) are fitted to the analytical expression, Eq. (12), yielding $\sigma/\tau=0.268\pm0.013$.

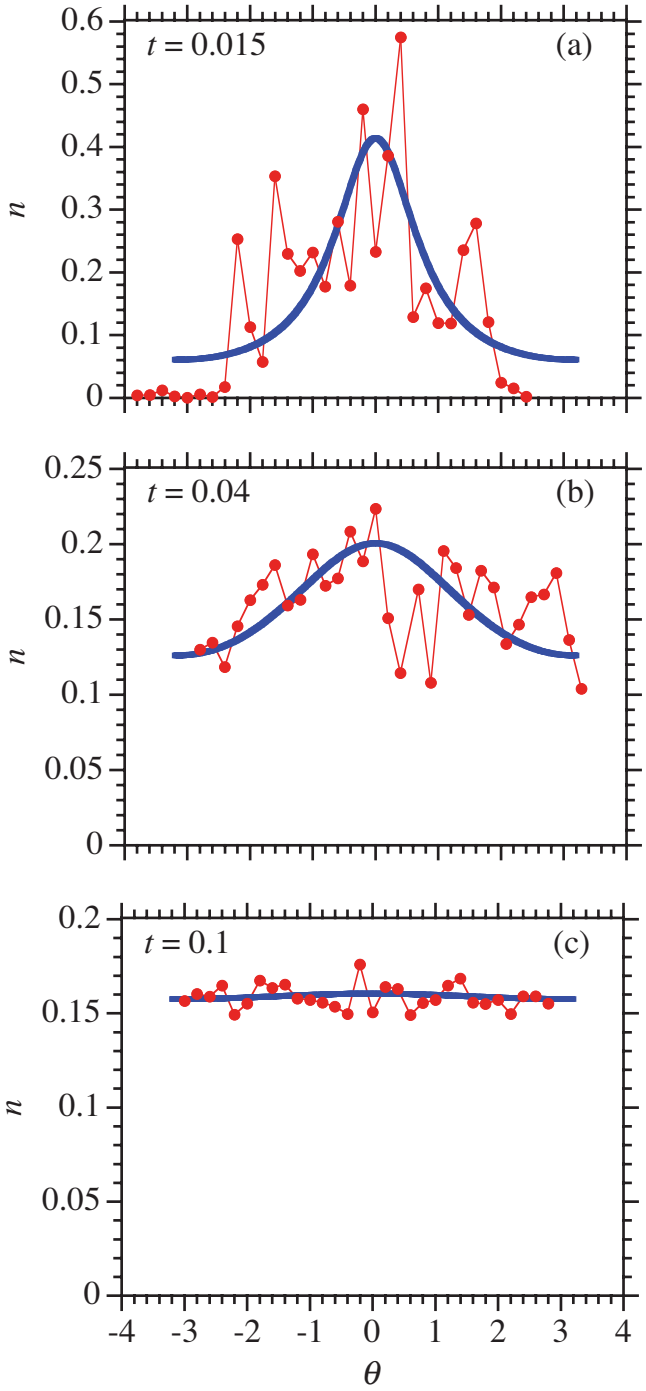

FIG. 4. (Color online) Comparison of the time evolution of the pdf of tracer particles with fixed initial toroidal velocity $V_0=400\pi$, and the analytical expression, Eq. (6).

of the random velocity initialization of the tracers. What may be surprising is the change of the functional form of the distribution. These distributions do not look at all like the analytical distributions given by Eq. (6).

The explanation is simple. With a single initial velocity for all particles, at any given time they were all located at the same toroidal angle. Now, with the random initial velocities, at any given time the particles are distributed over a range of toroidal angles and what we have measured is a poloidal

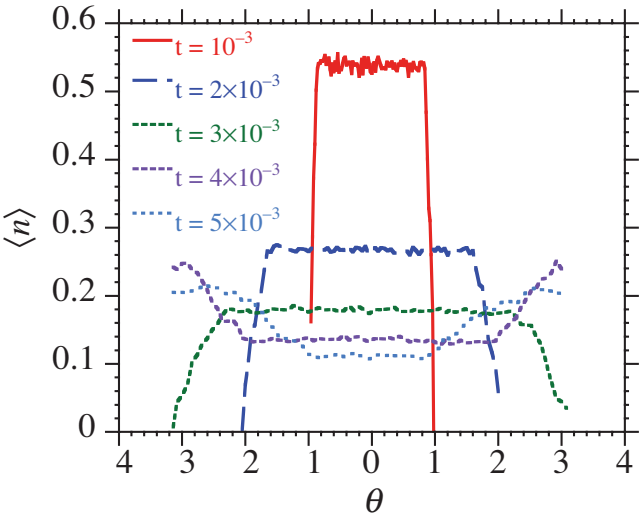

FIG. 5. (Color online) Numerical computation of the time evolution of the pdf of tracer particles with random initial toroidal velocities.

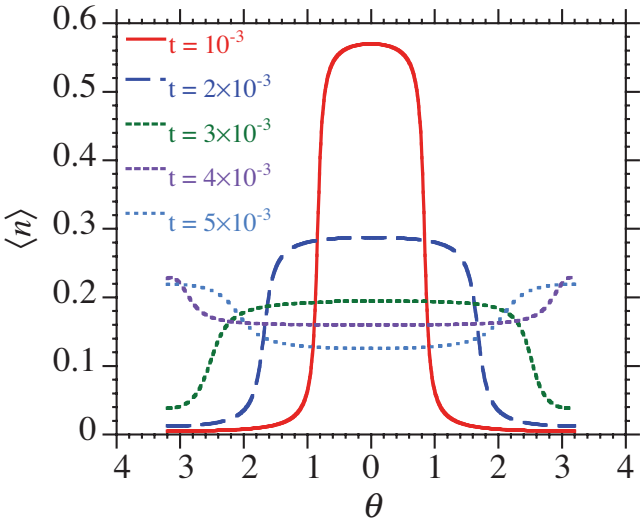

FIG. 6. (Color online) Time evolution of $n(\theta,t)$ given by Eq. (14) for the values of the parameters corresponding to the case plotted in Fig. 5.

distribution averaged over all the toroidal angles. Furthermore, since there is a mean drift associated with the twist of the magnetic field lines, in each toroidal plane ζ, the poloidal distribution has its peak at a different value of θ. In each toroidal plane ζ, the analytical distribution is given by Eq. (6) with values a given value of ζ in the range $[-V_{\max}t, V_{\max}t]$. Here $V_{\max}=400\pi$ is the maximum velocity of the tracers. Therefore, to reproduce the measured poloidal distribution, we have to average the fixed ζ distribution over the toroidal angle, that is

$$\langle n\rangle(\theta,t) = \frac{1-e^{-2\sigma t/\tau}}{2\pi}\frac{1}{2V_{\max}t} \times \int_{-V_{\max}t}^{V_{\max}t} \frac{d\zeta}{1-2e^{-\sigma t/\tau}\cos(\theta-u\zeta)+e^{-2\sigma t/\tau}}, \quad (13)$$

where u is the average pitch of the field line at the radial position of the initial tracers. After some algebra, one obtains

$$\langle n\rangle(\theta,t) = \frac{1}{2\pi u V_{\max}t}\left\{\arctan\left[\frac{1+e^{-\sigma t/\tau}}{1-e^{-\sigma t/\tau}}\tan\left(\frac{\theta+uV_{\max}t}{2}\right)\right] - \arctan\left[\frac{1+e^{-\sigma t/\tau}}{1-e^{-\sigma t/\tau}}\tan\left(\frac{\theta-uV_{\max}t}{2}\right)\right]\right\}. \quad (14)$$

This distribution should correspond to the one obtained in the numerical calculations. Using the value of α obtained from the previous section and the following estimate for $uV_{\max}$, $u=2/3$ and $V_{\max}=400\pi$ as used in the numerical calculations, we have plotted the corresponding pdfs in Fig. 6. The agreement between Figs. 5 and 6 is very good. For the randomized velocity case, once we have averaged over the initial velocities, there is no difference between anomalous diffusion with $\alpha=1$ and pure ballistic motion of the particles in the absence of the flow structures. However, the distinction is clear when we look at monoenergetic particles, as we saw at the beginning of this section.

IV. CONCLUSIONS

In this paper, we have used numerical simulations of resistive ballooning mode turbulence at low beta (sufficiently so to produce a topological instability) to illustrate the adequacy of recent periodic formulations of fractional transport equations[5] to describe nondiffusive turbulent transport in the poloidal direction. The formalism is quite general and could be easily applied to many other instances of transport problems along a periodic direction, of which parallel equilibration dynamics in toroidal magnetic devices is just one example.

In the case examined here, nondiffusive transport ensues due to the complex topology of the potential isosurfaces present in the system, a direct consequence of the narrow spectral band of dominant modes. Both radial and poloidal transport exhibit nondiffusive features due to this complex topology, but their physical origin is rather different, as explained in the text. The radial anomalous diffusion in this system was already considered in Ref. 13. In the current paper, we have focused instead on the poloidal transport, which turns out to be an interesting example of $\alpha=1$ anomalous diffusion. The origin of this value of α is in the fact that, away from the streamers, particles simply spread out ballistically along the filaments while on the high-field side. Once they reach the low-field side again and enter a new streamer structure, their direction of motion can be modified as the new streamer breaks up to form a new set of filaments towards the high-field side and particles get trapped in them. It is this combination of ballistic motion plus scattering of velocity directions which is ultimately responsible of a Cauchy type (i.e., $\alpha=1$) diffusive process.

By looking in detail at the poloidal distribution of monoenergetic particle tracers, we have also shown that the new mathematical framework can capture the features of the poloidal transport process. There is very good agreement between numerical results and the analytical calculation describing this phenomenon.[5] If tracers with random velocities

are used, once we average over initial conditions, it is not possible to distinguish the anomalous diffusion with $\alpha=1$ from the normal ballistic motion of the particles in the absence of the flow structures.

ACKNOWLEDGMENTS

This research was sponsored by the DGICYT (Dirección General de Investigaciones Científicas y Tecnológicas) of Spain under Project Nos. ENE2004-04319 and ENE2006-15244-C03-01 and by CM-UC3M (Comunidad de Madrid—Universidad Carlos III) Project No. CCG06-UC3M/ESP-0815. Part of this research was sponsored by the Laboratory Research and Development Program of Oak Ridge National Laboratory, managed by UT-Battelle, LLC, for the U.S. Department of Energy under Contract No. DE-AC05-00OR22725. L.G. acknowledges the financial support of Secretaría de Estado de Universidades e Investigación of Spain during his stay at Oak Ridge National Laboratory.

APPENDIX: LÉVY SKEW ALPHA-STABLE DISTRIBUTIONS

The family of *Lévy skew alpha-stable distributions* (or simply *stable distributions*, or *Lévy distributions*) is parameterized by four real numbers $\alpha\in(0,2]$, $\beta\in[-1,1]$, $\sigma>0$, and $\mu\in\mathbb{R}$. Their characteristic function (i.e., their Fourier transform) is given by[14]

$$\hat{S}(\alpha,\beta,\sigma,\mu)(k)=\begin{cases}\exp\left\{-\sigma^{\alpha}|k|^{\alpha}\left[1-i\beta\,\mathrm{sign}(k)\tan\left(\frac{\pi\alpha}{2}\right)\right]+i\mu k\right\} & \alpha\neq 1,\\ \exp\left\{-\sigma|k|\left[1+i\beta\frac{2}{\pi}\,\mathrm{sign}(k)\ln|k|\right]+i\mu k\right\} & \alpha=1.\end{cases} \tag{A1}$$

According to the generalized central limit theorem,[14] stable distributions are the only possible distributions with a domain of attraction. The index α is related to the asymptotic behavior of $S(\alpha,\beta,\sigma,\mu)(x)$ at large x,

$$S(\alpha,\beta,\sigma,\mu)(x)=\begin{cases}C_{\alpha}\left(\frac{1-\beta}{2}\right)\sigma^{\alpha}|x|^{-1-\alpha} & x\to-\infty,\\ C_{\alpha}\left(\frac{1+\beta}{2}\right)\sigma^{\alpha}|x|^{-1-\alpha} & x\to\infty,\end{cases} \tag{A2}$$

for $\alpha\in(0,2)$. For $\alpha=2$, $S(2,\beta,\sigma,\mu)$ is a Gaussian distribution.

[1] L. Garcia, B. A. Carreras, and V. E. Lynch, Phys. Plasmas **9**, 47 (2002).
[2] B. A. Carreras, V. E. Lynch, L. Garcia, M. Edelman, and G. M. Zaslavsky, Chaos **13**, 1175 (2003).
[3] G. M. Zaslavsky, B. A. Carreras, V. E. Lynch, L. Garcia, and M. Edelman, Phys. Rev. E **72**, 026227 (2005).
[4] B. A. Carreras, D. Newman, V. E. Lynch, and P. H. Diamond, Phys. Plasmas **3**, 2903 (1996).
[5] I. Calvo, B. A. Carreras, R. Sánchez, and B. P. van Milligen, J. Phys. A **40**, 13511 (2007).
[6] E. W. Montroll and G. Weiss, J. Math. Phys. **6**, 167 (1965).
[7] H. Scher and M. Lax, Phys. Rev. B **7**, 4491 (1973).
[8] J. W. Connor, R. J. Hastie, and J. Taylor, Proc. R. Soc. London, Ser. A **365**, 1 (1979).
[9] M. S. Chance, R. L. Dewar, E. A. Frieman, A. H. Glasser, J. M. Greene, R. C. Grimm, S. C. Jardin, J. L. Johnson, J. Manickam, M. Okabayashi, and A. M. M. Todd, *Proceedings of the 7th International Conference on Plasma Physics and Controlled Nuclear Fusion Research*, Innsbruck, Austria, 1978 (IAEA, Vienna, Austria, 1979), Vol. I, p. 677.
[10] H. R. Strauss, Phys. Fluids **20**, 1354 (1977).
[11] J. F. Drake and T. M. Antosen, Jr., Phys. Fluids **27**, 898 (1984).
[12] G. M. Zaslavsky and M. Edelman, Chaos **11**, 295 (2001).
[13] L. Garcia and B. A. Carreras, Phys. Plasmas **13**, 022310 (2006).
[14] G. Samorodnitsky and M. S. Taqqu, *Stable Non-Gaussian Processes* (Chapman & Hall, New York, 1994), p. 5.